

# Knots in Charged Polymers

Paul G. Dommersnes,<sup>1,2,\*</sup> Yacov Kantor,<sup>3,1,†</sup> and Mehran Kardar<sup>1</sup>

<sup>1</sup>*Department of Physics, Massachusetts Institute of Technology, Cambridge, Massachusetts 02139*

<sup>2</sup>*Department of Physics, Norwegian University of Science and Technology, 7491 Trondheim, Norway*

<sup>3</sup>*School for Physics and Astronomy, Tel Aviv University, Tel Aviv 69978, Israel*

(Dated: October 25, 2018)

The interplay of topological constraints and Coulomb interactions in static and dynamic properties of charged polymers is investigated by numerical simulations and scaling arguments. In the absence of screening, the long-range interaction localizes irreducible topological constraints into tight molecular knots, while composite constraints are factored and separated. Even when the forces are screened, tight knots may survive as local (or even global) equilibria, as long as the overall rigidity of the polymer is dominated by the Coulomb interactions. As entanglements involving tight knots are not easy to eliminate, their presence greatly influences the relaxation times of the system. In particular, we find that tight knots in open polymers are removed by diffusion along the chain, rather than by opening up. The knot diffusion coefficient actually decreases with its charge density, and for highly charged polymers the knot's position appears frozen.

PACS numbers: 02.10.Kn 82.35.Rs 87.15.-v 36.20.Ey 05.40.-a

## I. INTRODUCTION

A polymer chain can be easily deformed, but since it cannot cross itself, it is subject to topological constraints. These constraints can be temporary, such as entanglements between linear polymers, or permanent if the chains are closed (ring polymers) or cross-linked. Understanding the influence of topological entanglements on static and dynamic properties of polymers is a long-standing issue [1, 2], which has recently found renewed interest in the context of *knotted biopolymers*. DNA in the cell can change its topology by the *topoisomerase* enzymes that pass one strand through another, in the process either creating or removing knots [3]. Synthetic RNA trefoil knots have been used to prove the existence of a similar (previously unknown) topology changing enzyme [4]. There is also much interest in developing artificial biopolymers, for example as molecular building blocks or for DNA-based computing, and in this quest complex knots and links have been created in both *single* and *double* stranded DNA [5]. Tight knots have been tied in single molecule experiments on both DNA and actin filaments using optical tweezers [6].

Several theoretical approaches have addressed the influence of topological constraints in polymer networks and solutions. In particular, the *tube* model [2] in which the constraints are replaced by a hard confining tube, is quite successful in predicting relaxation dynamics of polymeric solutions. In a complementary approach, topological constraints are described in terms of *localized* entanglements or knots, that perform collective motions along the polymers [7]. Single molecule experiments are now able to probe polymers of specified topology, and to

examine the influence of knot complexity on basic physical properties such as the radius of gyration  $R_g$ . A simple scaling picture [8] suggests that  $R_g$  is reduced as a power of the knot complexity, measured by the minimal number of crossings in a projection. Indeed, a Flory mean field theory of knotted ring polymers [9, 10] incorporating this knot invariant predicts various scaling dependences on knot complexity. A topological localization effect is also suggested, in which knots segregate in a single relatively compact domain while the rest of the polymer ring expels all the entanglements and swells freely. Recent Monte Carlo simulations in Refs. [11, 12, 13, 14] support the idea that entropic factors localize topological constraints. This is bolstered by analytical arguments on slip-linked polymers [15], and experiments on vibrated granular chains [16].

Many biopolymers are highly charged. The effect of electrostatics on knotting probability of double stranded DNA has been studied in the case where the screening length is smaller than the persistence length of the polymer. The effect of the Coulomb interactions is then to renormalize the effective thickness of the polymer [17, 18]. However synthetic polymers and single stranded DNA both have an intrinsic persistence length of the order  $\ell_p \sim 1\text{nm}$  [19] which could be small compared to the electrostatic screening lengths. In this paper we explore the influence of topological constraints on charged polymers in cases where the screening length is large or comparable to the intrinsic persistence length. In Sec. II we start by considering the idealized case of unscreened Coulomb interactions. This case demonstrates that under long-range interactions the topological constraints are pulled into tight knots. As discussed in Sec. III, this conclusion has to be re-examined in real systems due to finite rigidity of the polymer, thermal fluctuations, and, most importantly, finite screening. Surprisingly, we find that tight knots are rather resilient: They remain as global equilibrium solutions as long as the overall shape of the

\*Electronic address: paul.dommersnes@phys.ntnu.no

†Electronic address: kantor@post.tau.ac.il

polymer is dominated by the (screened) Coulomb interactions. Tight knots can also remain as metastable states for shorter screening lengths, as long as the electrostatic bending rigidity is larger than the intrinsic one. Such long-lived tight knots have strong influence on the relaxation dynamics of the polymers as discussed in Sec. IV. In particular, we find that the most likely way for eliminating topological entanglements is by diffusion of tight knots along the chain; interestingly stronger Coulomb interactions lead to tighter knots that are less mobile.

## II. UNSCREENED INTERACTIONS

We first consider a simple model of a charged polymer in which monomers repel each other via *unscreened* Coulomb interactions. The interaction between two charges  $e$ , in a solvent with dielectric constant  $\epsilon$ , separated by distance  $r$  is  $e^2/\epsilon r$ , and consequently the overall electrostatic energy of a polymer of  $N$  monomers is  $V_c = (e^2/\epsilon) \sum_{i>j}^N 1/|\mathbf{r}_i - \mathbf{r}_j|$ , where  $\mathbf{r}_i$  is the position of  $i$ -th monomer. Given a typical separation between adjacent monomers of  $a$ , it is convenient to introduce the energy scale  $\epsilon_o \equiv e^2/\epsilon a$ . Initially, we focus on configurations in which the monomers are locally stretched to form smooth straight segments, gradually curving at a larger length scale  $R$  set by the overall shape. For such configurations the Coulomb energy has the form

$$E_c(N) = \epsilon_o \left[ N \ln \left( \frac{R}{a} \right) + c \frac{aN^2}{R} \right], \quad (1)$$

where  $c$  is a numerical constant of order unity, and we note the following:

- For any smooth curve, the integral of the  $1/r$ -potential leads to a logarithmic divergence, and consequently the energy of the polymer is *overextensive*, and, consequently, the tension on the polymer increases as  $\ln N$ . Therefore, thermal fluctuations are irrelevant for a sufficiently long polymer, whose shape is determined by minimizing the energy.
- The second term in Eq. 1 can be regarded as the Coulomb interaction between charges (or order  $N$ ) on remote parts of the polymer (distances of order  $R$ ). Since typically  $R \propto Na$ , the partition of the energy between the two parts is not precise, and can be changed by redefining  $R$ .
- The Coulomb interaction prefers to keep the charges far apart, and the polymer minimizes its energy by assuming a shape with maximal  $R$ . Thus, open polymers simply form straight lines, while unknotted ring-polymers form circles.

The above argument can be misleading in the case of a knotted polymer, as illustrated in Fig. 1. Here, we used Monte Carlo (MC) off-lattice simulations to determine

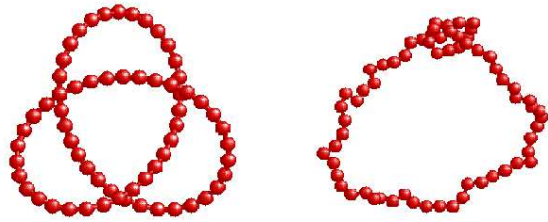


FIG. 1: The initial (left) and equilibrium (right) conformations of a 64-monomer charged polymer, at  $\tilde{T} = 1.4$ , forming a trefoil knot. (The right figure is reduced by a factor of 2).

the shape of knotted polymers at finite temperature. Our model polymer consisted of hard sphere monomers connected by “tethers” [20] that have no energy but limit the distance of a connected pair to 1.05 of the hard sphere diameter  $a$ . Fig. 1 depicts the results of a simulation for a trefoil knot: As an initial conformation (left) in this simulation (as well as in the subsequent simulations of more complex knots) we used a harmonic representation [21] in which coordinates of the monomers are given as polynomials in  $\cos(t)$  and  $\sin(t)$ , where  $t$  parametrizes the curve. (This provides a relatively clear visualization of the knot.) Since the hard core and tether potentials do not have an energy scale, the temperature  $T$  appears in the simulations in the combination  $k_B T/\epsilon_o$ , which we will denote as dimensionless temperature  $\tilde{T}$ . All simulations described in this section were performed for  $\tilde{T} = 1.4$ . It is customary to represent the strength of the electrostatic potential by the *Bjerrum length*  $\ell_B = e^2/\epsilon k_B T$ . (In water at room temperature  $\ell_B = 0.7\text{nm}$ .) In our notation, the Bjerrum length is simply related to the dimensionless temperature by  $\ell_B \equiv a/\tilde{T}$ . (Note that for the moderate values of  $N = 64$  used in this simulation, the polymer shape on the right of Fig. 1 is somewhat ‘wiggly’; an effect that should disappear for  $N \rightarrow \infty$  due to the overextensivity of the energy.)

Figure 1 clearly shows that in equilibrium the trefoil assumes an almost circular shape, with the topological details concentrated on a very small portion. (The scale of the right side part of Fig. 1 has in fact been reduced by a factor 2 relative to the left figure, and the actual linear extent of the equilibrated knot is almost twice its initial size.) This behavior can be explained by comparing the long and short-ranged contributions to the Coulomb interaction: By expanding its radius, the long-range part of the Coulomb energy is reduced by a factor of  $\delta(N^2/R) \propto N$ . This comes at the cost of bringing several charges close together in the tight portion, but the latter energy is independent of  $N$ , and can be easily tolerated for sufficiently long polymers.

Because of the highly curved portion, Eq. 1 does not apply to tight knots. For a semi-quantitative understanding of the tension that creates such objects, con-

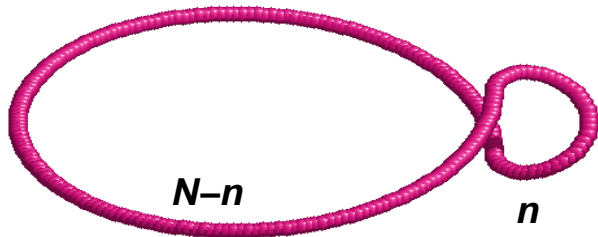


FIG. 2: A closed loop ( $N$ -monomer polymer) folded into a shape that can be approximately described as two circles consisting of  $N - n$  and  $n$  monomers, separated from each other by a distance of order  $n$  monomer sizes.

consider a simpler example of an  $N$ -monomer closed chain folded into a shape consisting of a large circle of  $N - n$  monomers, and a small loop of  $n$  monomers, as depicted in Fig. 2. For  $n \ll N$ , the electrostatic energy can be decomposed as  $E_c(N - n) + E_c(n) + E_i$ , where  $E_c$  is given in Eq. 1, while  $E_i$  is the interaction energy between the small loop and the large circle. Assuming that the curved strands are separated by a distance of the order  $na$ , the latter is of the order of  $2\epsilon_o n[\ln(N/n) + c']$ , where  $c'$  is a constant depending on the details of the shape. The leading  $n$ -dependent part of the total energy is then

$$E(N, n) \simeq \epsilon_o n \ln\left(\frac{N}{n}\right), \quad (2)$$

representing a tension that grows logarithmically with the length of the polymer. This conclusion is not limited to the shape depicted in Fig. 2, but should apply to any smooth linear curve consisting of two portions of very different sizes. Equation 2 thus indicates that from purely electrostatic energy considerations  $n$  should take the smallest possible value, as indeed happens in the case of a tight knot in Fig. 1.

The tightness observed for a trefoil knot also occurs in more complicated topologies. Figure 3 depicts the results of equilibration of 128-monomer polymers beginning from a harmonic shape on the left, to equilibrium shapes (on the right) at  $\tilde{T} = 1.4$ . Below each figure we indicate the type of the knot in the standard notation  $\mathcal{C}_k$ , where  $\mathcal{C}$  is the minimal number of crossings the knot can have in a planar projection [22]. Since for a given number of crossings there can exist several different knots, an additional subscript  $k$  labels the standard ordering of these knots. (For  $\mathcal{C} = 3$  and 4 there is only one knot, while for  $\mathcal{C} = 8$

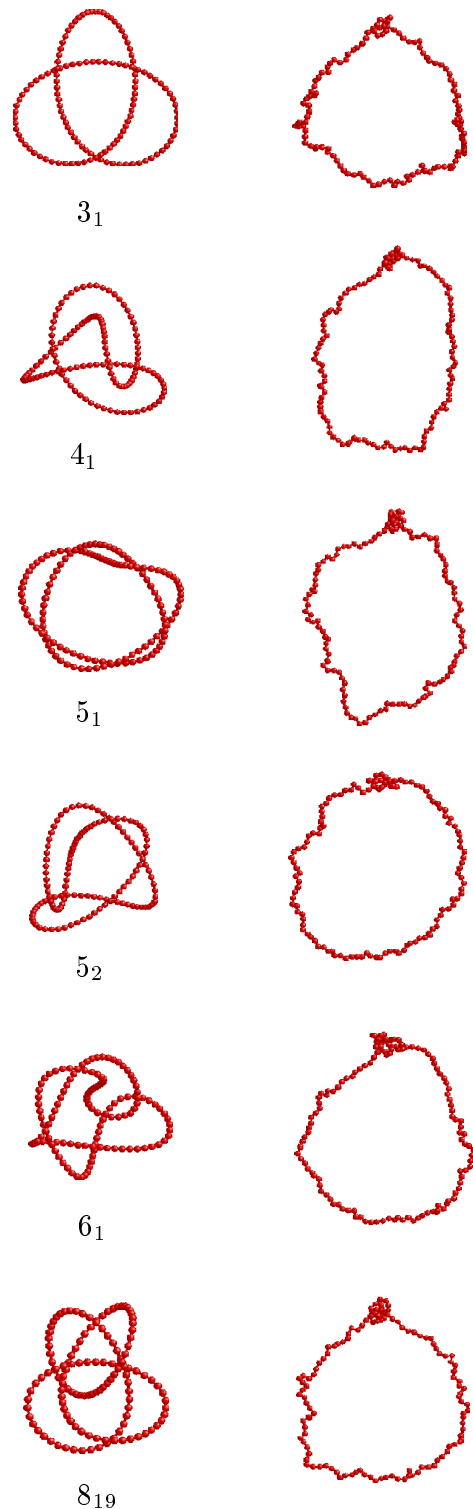


FIG. 3: The initial (left) and equilibrium (right) shapes of knots formed by 128-monomer polymers at  $\tilde{T} = 1.4$  ( $\ell_B = 0.7a$ ). A selection of prime knots of varying degrees of complexity is depicted. (The figures in the right column have been scaled down.) The numbers in the left column are the standard notations for knot types.

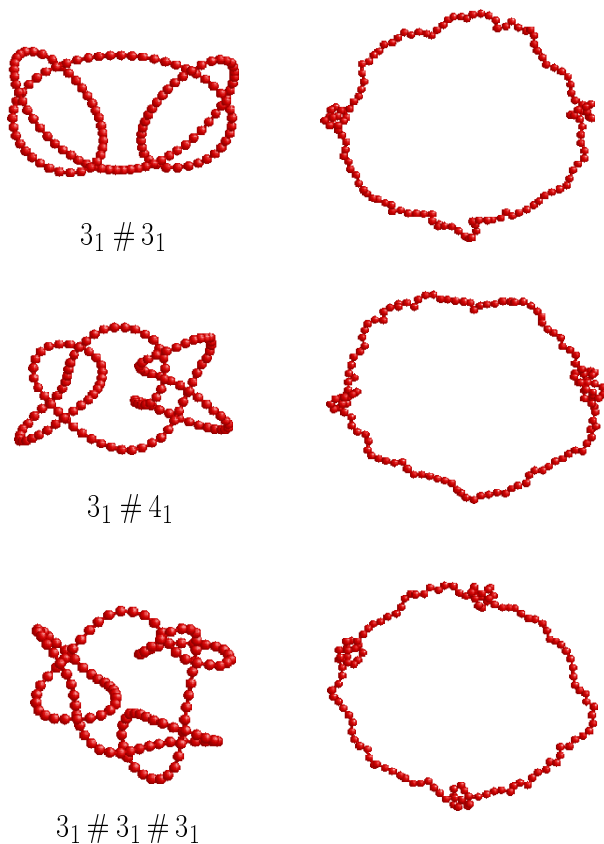


FIG. 4: “Coulomb factorization” of composite knots on a 128-monomer polymer at  $\bar{T} = 1.4$ . Original (left) and equilibrium (right) configurations (scaled down) are shown.

there are 21 distinct knots [22].) Despite the increasing topological complexity of the knots in Fig. 3, their eventual (collapsed-knot) state is reliably represented by the semi-quantitative description based on the energetics of Fig. 2.

The above arguments indicate the energetic advantage of compressing any *indivisible* topological constraint into a tight shape (as opposed to leaving it as an expanded structure). However, similar considerations suggest that, *if possible*, any concentrated region of charge should split into smaller elements placed as far as possible from each other. Such a reduction is not possible for the *prime knots* considered in Fig. 3, which (by definition) cannot be separated into several parts connected by a single line. In contrast, *composite knots* are formed by joining several prime factors together, and Fig. 4 presents initial and final (equilibrium) states of several such knots on 128-monomer polymers. The notation below each knot indicates its constituent prime components. The Coulomb interaction clearly “factorizes” any composite knot, separating its elements as far as possible. However, since the typical interaction energies between the prime factors are only a few  $\epsilon_o$ , thermal fluctuations ( $\bar{T} = 1.4$ ) in the dis-

tances between these tight regions are quite pronounced.

### III. BEYOND ‘IDEAL’ KNOTS

Many of the results in the previous section are in fact known to knot theorists, who have investigated long-range repulsive interactions with the aim of finding a knot-invariant energy [23, 24]. The basic question is whether a properly scaled energy of the ground state configuration (the *ideal* state) for certain choices of interaction functions can be used as a means of distinguishing different knot types. An example of such an interaction is Simon’s ‘minimal distance’ between the strands function, or a repulsive  $1/r^2$  type interaction [25] which produces symmetric spread out ground states. In Ref. [26] it was conjectured that minimizing knot-invariant energies should decompose a knot into prime sub-knots and simulations with  $1/r^2$  interactions support this [27]. Electrostatic interactions do not generate useful knot-invariant energies, since, in the absence of excluded volume interactions, knots on a continuous curve are collapsed to a point [28], providing no (cut-off independent) way of identifying knots. (Indeed, in the simulations of the previous section knots were tightened into compact objects whose extent was determined by the monomer size.) While this conclusion may be disappointing to a knot-theorist, it is encouraging from the perspective of polymer science, since it is easier to describe the properties of tight entanglements, without having to worry about their precise topology. However, this is the case only if we can demonstrate that tight knots survive for realistic polymers subject to electrostatic interactions in actual solvents. Accordingly, in this section we shall include additional attributes present in such situations, and consider the effects of bending rigidity, thermal fluctuations, and (most importantly) of a finite screening length. In these circumstances the size of the knot can be significantly larger than in its maximally tight state; nevertheless, tight knots can still remain.

#### A. Bending rigidity

Many microscopic aspects of polymers are captured at a mesoscopic scale by a curvature energy, describing its resistance to bending. In a charged polymer one should distinguish between the *intrinsic* bending rigidity, and an *effective* rigidity which includes the electrostatic contributions. The latter arises because bending a straight segment brings the monomers closer and thus increases the Coulomb energy. The former can be represented by a length  $\ell_p$  at which, in the absence of other interactions, the transverse thermal fluctuations of the polymer become of the same order as the length-scale itself, or at which orientations of the bonds become uncorrelated. Simple analysis relates  $\ell_p$  to the bending rigidity  $\kappa$  and temperature by  $\kappa \equiv k_B T \ell_p$ . In charged polymers,

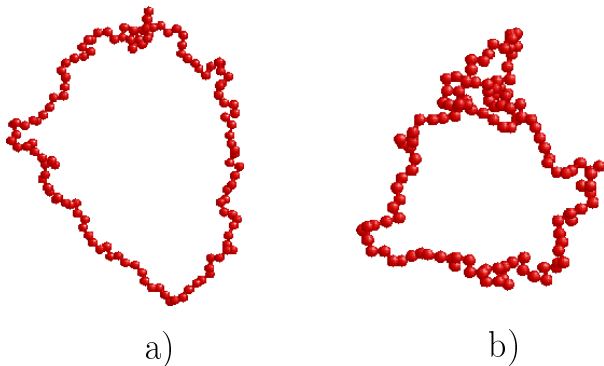


FIG. 5: Equilibrium configurations of a 128-monomer trefoil knot: (a) a tight ( $\sim 20$  monomer) knot at  $\tilde{T} = 5$ , and (b) an expanded ( $\sim 60$  monomer) knot at  $\tilde{T} = 10$ .

$\ell_p$  should be measured in the presence of high salt content, so that electrostatic contributions to rigidity are screened out. It is reasonable that the bending rigidity, rather than monomer size, should determine the size of a tight knot. The energy for bending a segment of length  $\ell$ , with radius of curvature also of order of  $\ell$ , is  $\kappa/\ell$  with a dimensionless shape-dependent prefactor. For the shape depicted in Fig. 2, there is now a bending cost of  $E_b \approx \kappa/na$  which competes with the electrostatic energy in Eq. 2. By minimizing the sum of these energies, we find that the optimal knot size is

$$\begin{aligned} n_k &\approx \sqrt{\frac{\kappa}{\epsilon_o \ln(N/n_k)}} \approx \sqrt{\frac{\kappa}{\epsilon_o \ln(N^2 \epsilon_o / \kappa)}} \\ &= \sqrt{\frac{\ell_p}{\ell_B \ln(N^2 \ell_B / \ell_p)}}, \end{aligned} \quad (3)$$

where we have omitted numerical prefactors of order unity. This result indicates that the knot in stiff polymers of moderate size  $N$  can be as large as  $\sqrt{\kappa/\epsilon_o} = \sqrt{\ell_p/\ell_B}$ , and becomes compact only for  $N \sim \exp(\kappa/\epsilon_o)$ .

### B. Thermal Fluctuations

At high temperatures, entropic factors (which favor crumpled states) compete with electrostatic effects. While the latter dominate on sufficiently long length-scales, at short length-scales fluctuations are important. This competition can be visualized by a simple *blob* picture [1]. If a strong external force  $f$  is applied to a self-avoiding polymer without electrostatic interactions, it is stretched to a linear form. This linear object, however, has a finite width  $R_b$ , and can be regarded as a chain of blobs of this size. On length-scales shorter than the blob size, the external force has negligible effect, and we can relate  $R_b$  to the number of monomers  $N_b$  forming the blob via the usual relation for self-avoiding polymers[1]:

$R_b \approx aN_b^\nu$  with  $\nu \approx 0.59$ . Consequently, the linear extent of the entire polymer is approximately  $R_b(N/N_b)$ . If a weak force  $f$  is applied to a segment of spatial extent  $R_b$ , that segment is stretched[1] by an amount  $X \approx R_b^2 f/k_B T$ . The size of a blob is determined by requirement that  $X \approx R_b$ , leading to  $R_b \approx k_B T/f$ . An open charged polymer can also be viewed as a stretched chain formed from such blobs [29, 30], while a ring-polymer is a circle of such blobs. The force stretching a blob in an object of this type is  $\epsilon_o a(N_b/R_b)^2 \ln(N/N_b)$ . By substituting this force into the expression for blob size, and solving it, we extract the number of monomers in each blob as

$$\begin{aligned} N_b &\approx \left[ \frac{k_B T}{\epsilon_o \ln(N/N_b)} \right]^{\frac{1}{2-\nu}} \approx \left[ \frac{\tilde{T}}{\ln(N/\tilde{T}^{\frac{1}{2-\nu}})} \right]^{\frac{1}{2-\nu}} \\ &= \left[ \frac{a/\ell_B}{\ln N(a/\ell_B)^{\frac{1}{2-\nu}}} \right]^{\frac{1}{2-\nu}}. \end{aligned} \quad (4)$$

Of course, the blob picture is meaningful only if  $N_b$  is larger than unity. Thus blobs can appear only for temperatures  $\tilde{T} \gg \ln N$ ; and for  $N = 128$  we expect to see the blobs for  $\tilde{T} \gtrsim 5$ . Fig. 5 depicts equilibrium shapes of a trefoil knot at  $\tilde{T} = 5$  and  $\tilde{T} = 10$ , and we see the appearance of a wiggly structure in the higher temperature regime. At such high temperatures, we expect knots to have a size typical of that in a non-charged polymer consisting of  $N_b$  monomers. The exact size of the knot region in non-charged polymers in three-dimensional space is not known; simulations suggest that knots are localized [12, 13], but not compact [14]. The size of the blob in Fig. 5 is too small for any kind of quantitative study, but we clearly see that the knot is no longer maximally compact.

### C. Screened Interactions

A charged polymer in solution is accompanied by neutralizing counterions, and potentially other charged ions due to added salt. In general, the effect of these additional ions on the charged polymer is quite complicated, and dependent on the intrinsic stiffness, strength of the charge, and valency of counterions [31]. However, in many cases the net effect can be approximated by a screened Coulomb potential  $V = (e^2/\epsilon r) \exp(-r/\lambda)$ , where  $\lambda$  is the Debye screening length [32]. Since the previous arguments for the tightness of charged knots rely on the long-ranged part of the Coulomb interaction, we may well question if and when tight knots survive with screened forces.

It is important to realize that Coulomb interactions affect the polymer on scales much larger than  $\lambda$ , due to increased bending rigidity. Curving a straight polymer to a radius  $R$  brings its charges closer, resulting in an extra energy cost of order  $(e^2/\epsilon R)\tilde{\lambda}^2$  for screened Coulomb interactions, where  $\tilde{\lambda} \equiv \lambda/a$  is the reduced

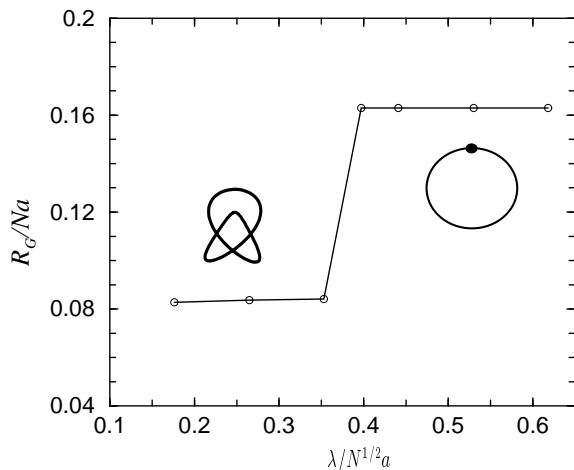


FIG. 6: Radius of gyration,  $R_g$ , of the ground state configuration of a trefoil knot, as a function of the screening length  $\lambda$  for a 128-monomer polymer.  $R_g$  has been normalized by the length of the polymer  $Na$ .

screening length. This can be regarded as an effective bending rigidity, which (in the presence of thermal fluctuations) leads to the Odijk–Skolnick–Fixman persistence length [33] of  $\ell_c = \lambda^2 e^2 / (\varepsilon k_B T a^2) = \ell_B \tilde{\lambda}^2$ . The electrostatic persistence length is in general much larger than the screening length. In terms of our reduced variables  $\tilde{\ell}_c \equiv \ell_c / a = \lambda^2 / T$ . This expression is valid provided that the length scales considered are larger than the screening length, and  $\tilde{T} < \tilde{\lambda}$ .

For very large  $\lambda$ , comparable to the size of the polymer, the effects of screening are not very important: E.g., Eq. 2 for electrostatic energy of a knot remains valid if  $N$  is replaced by  $\tilde{\lambda}$ , and similar replacements should be made in Eq. 3 for the knot size in a stiff polymer, or in Eq. 4 for the blob size. In all these expressions, the number of monomers enters only in a logarithm, and, consequently, its replacement by  $\lambda$  does not significantly change the result. Eq. 3 for the optimal knot size is valid (with  $N$  replaced by  $\tilde{\lambda}$ ) only if the knot is smaller than the screening length. This condition,  $\lambda > an_k$ , leads to the cross-over boundary

$$\lambda > a \sqrt{\frac{\ell_p}{\ell_B}}, \quad (5)$$

which is equivalent to  $\ell_c > \ell_p$ . We thus conclude that a tight knot can exist only when the overall bending rigidity is dominated by electrostatic contributions. For smaller values of  $\lambda$ , the short range repulsion can no longer bend the knot into a tight shape.

Note that the analysis leading to Eq. 3 only demonstrates the local stability of a tight knot. The global energy minimum could still occur for a spread out configuration. To decide on the latter requires estimates of the energy difference between the two configurations, and depends on microscopic details, as well as the length of

the polymer. A circle with a tight knot, and the spread out knotted shape, both have a bending energy (at large scales) of the order of  $k_B T \ell_c / R$ . Since the circular shape has a larger radius, it has a lower energy, the energy difference scaling as  $k_B T \ell_c / (Na)$ , if both radii are proportional to the polymer length. The tight knot in the former has an additional local energy cost, which is of the order of  $k_B T (\ell_B / a)$  (possibly with logarithmic corrections), but independent of  $N$ . Thus, we expect the configuration with a spread-out knot to have a lower energy only for  $\ell_c / N < \ell_B$ , i.e. for screening lengths

$$\lambda \leq \lambda_c \approx a \sqrt{N}. \quad (6)$$

Note that the limiting value of  $\lambda$  still corresponds to a persistence length of the order of the extended polymer, i.e. the polymer shape is determined by energy considerations, and thermal fluctuations have little effect, at this point. We verified this conclusion by numerically determining the shape of the trefoil that minimizes the screened Coulomb interactions. Figure 6 shows the radius of gyration as a function of the screening length. For screening lengths larger than  $\lambda_c \sim 0.4aN^{1/2}$ , the knot switches from a loose to a tight configuration.

Let us briefly explore the possibility of tight knots in nucleic acids. Double stranded DNA has a bare persistence length of  $\ell_p \sim 50\text{nm}$ , which is much larger than typical screening lengths, and consequently is not likely to incorporate any knots tightened by Coulomb interactions. However, measurements on *single stranded* DNA in high salt concentrations [19] suggest a much smaller intrinsic  $\ell_p \sim 1\text{nm}$ , and presumably a similar (or smaller) value applies to single stranded RNA. Tight knots should then occur for single stranded nucleic acids for reasonable screening lengths of the order  $\lambda \sim 10\text{nm}$ . This could for example be relevant to the experiments of Ref. [4], where artificial knots in single stranded RNA were used to demonstrate the existence of a topology changing enzyme. Knotted polymers are often distinguished from unknotted ones by electrophoresis [4]. However, if the knot is tight, the knotted polymer may have an electrophoretic mobility close to that of a ring polymer, making such detection problematic.

#### IV. TIGHT KNOTS AND DYNAMICS

Tight knots are created whenever a polymer is under tension; the source of tension need not be long-range repulsions. For example, it has been argued that tight molecular knots appear in polymer systems undergoing crystallization, as crystallization at one point may create tension in other parts of the chain [34]. Polymers in a strong shear flow are also subject to tension [34, 35], and may even undergo a coil-stretch transition as a result [36]. It is plausible that stretching could tighten loose knots in the chain. Once created, such molecular knots should be quite stable and thus account for long-time memory



effects observed in polymer melts [34]. However, molecular dynamics simulations suggest that once the tension is removed a tight knot opens up in a short time [37]. Without being systematic, here we examine a couple of dynamical issues pertaining to charged tight knots, namely their creation in a high temperature quench, and their relaxation by diffusion along the chain.

### A. Tightening by Quench

It is quite likely that when topological entanglements are first formed, e.g. in the process of cyclization of a polymer, they are spread out over the whole chain. Subsequent tightening then occurs upon increasing tension. In the case of charged knots, this process is illustrated in Fig. 7. Here, the initial configurations are the spread out harmonic representations, which soon evolve into loops separated by tight elements. The relaxation process then slows down as one of the loops grows at the expense of the others. A universal last stage is the appearance of a structure reminiscent of Fig. 2, with two loops separated by a tight ‘slip-link.’ We observed the same sequence in simulations where the initial configuration was an equilibrated (random walk) knot. The formation of the two loops separated by a slip-link was again relatively fast, and the rate limiting step was the sliding of one loop through the tightly packed monomers at the slip-link.

### B. Diffusion of Tight Knots

As demonstrated in the previous situation, tight knots slow down the relaxation of the polymer to its eventual equilibrium state. Here we study such relaxation more explicitly for a knot in an open charged polymer. In this case there is no topological constraint, and the polymer is expected to unknot to achieve its equilibrium state. Does a tight knot in an open chain relax by becoming loose and opening up, or by sliding (diffusing) to one end. As demonstrated in Fig. 8, the latter is the case: The initial configuration (in a chain of  $N = 64$  monomers with unscreened interaction) remains tight, indicating that the stretching force from the monomers at the ends of the chain is larger than from those forming the knot. In the simulation, the knot’s position fluctuates for some time in the middle, before moving to one direction. The eventual unknotting occurs when the diffusing tight knot reaches the end of the polymer.

A tight knot in the middle of an open chain is in a meta-stable state. We can estimate a potential energy for the tight knot by considering a charge  $Q = ne$  along a charged chain of  $N$  monomers. The Coulomb energy then depends on the position of this charge  $N_1$ , as  $E = k_B T (\ell_B/a) n \ln[N_1(N - N_1)]$ . This energy is minimal when the charge  $Q$  is at either endpoint of the polymer, i.e. for  $N_1 = 0$  or  $N$ . Note that the force pushing the extra charge towards the end scales with  $\ell_B$ , and we

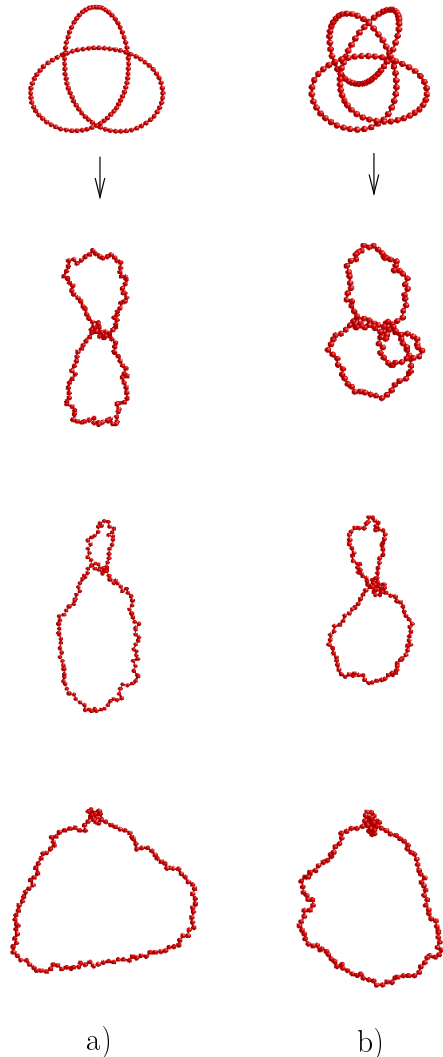


FIG. 7: Time evolution (using Monte Carlo dynamics) of (a)  $3_1$  and (b)  $8_{19}$  knots, from the initial (harmonic) geometry (top) through an intermediate state when the knot “strangles” the loop close its middle, and to a final state (bottom) when the knot is localized. A similar sequence takes place for all other prime knots in the simulations of Fig. 3.

may naively expect that the resulting relaxation becomes faster as the Coulomb energy is increased. In fact, the opposite occurs for charge knots, with relaxation slowing down as Coulomb interactions become more dominant. The reason is that increased charging energy leads to a higher tension and more closely packed monomers in the knot. Any motion of the knot requires some internal rearrangements of these monomers, accompanied by pulling in some monomers from the straight portions of the chain. This necessitates overcoming an energy barrier of  $\sim \ell_B \ln N$ , and consequently higher charged knots

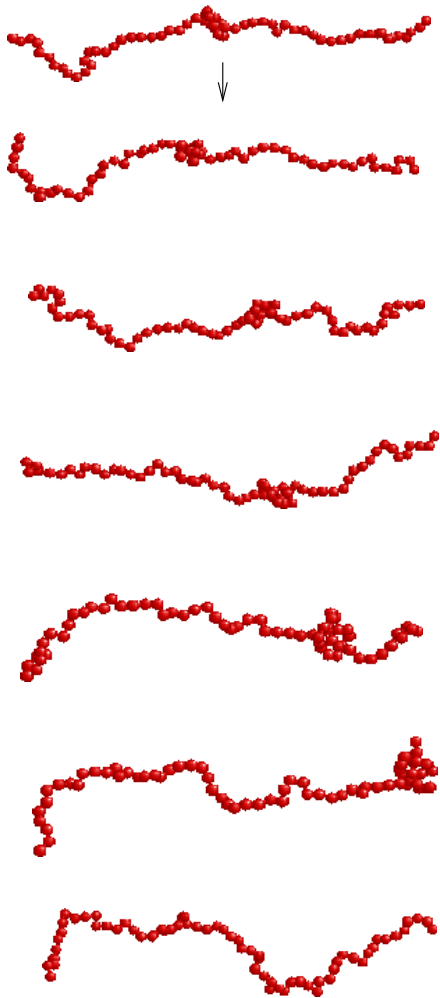


FIG. 8: Unknotting of a charged polymer with  $N = 64$  monomers and unscreened Coulomb interaction of strength  $\bar{T} = 1.4$  ( $\ell_B = 0.7a$ ). The initial configuration is a tight knot in the middle of the chain. Rather than open up gradually, the knot slides along the polymer and remains localized until it reaches the end.

are tight and harder to move. Since rearrangements require a large activation energy, the knot remains stuck in position. This is quite similar to what happens to a knot in a polymer under strong tension [34].

While with unscreened Coulomb interactions the tight knot feels a potential that drives it to one end, there is no such force when the interactions are screened (unless the distance between the knot and the endpoint of the polymer is of the order of the screening length). The energy barrier preventing the loosening of the knot is also finite in this case. The resulting dynamics for a chain of 128 monomers with a screening length of  $\lambda = 6a$  is demonstrated in Fig. 9; despite the screening the knot remains tight until it diffuses to one end. The characteristic time

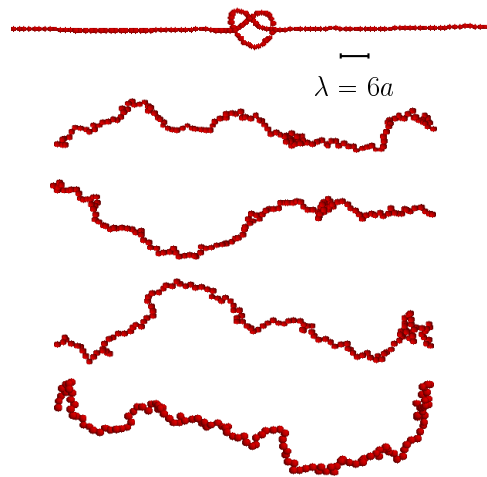


FIG. 9: Monte Carlo dynamics of a tight knot in a chain with  $N = 128$  monomers and screened interactions. The screening length is  $\lambda = 6a$ , roughly the size of the knot. The knot shows no sign of opening up, it remains tight till it reaches the end of the polymer.

scales for the relaxation of the knot can be estimated as follows. The time for diffusion over a distance  $Na$  scales as  $a^2 N^2 / D_{knot}$ , with the knot diffusion coefficient behaving as  $D_{knot} \propto D \exp(-\mathcal{E}_D / k_B T)$ . Here,  $D$  is the diffusion constant for a single monomer, while the activation energy for local rearrangements necessary for motion of the tight region is roughly  $\mathcal{E}_D \approx k_B T (\ell_B / a) \log(\lambda / a)$ . There is also the possibility that the knot becomes loose, escaping the local minimum of the tight configuration. The energy barrier for the latter is  $\mathcal{E}_b \approx k_B T \ell_B \lambda / a^2$ , with a corresponding time scale of  $\tau \approx (a^2 / D) \exp(\mathcal{E}_b / k_B T)$ . In time  $\tau$ , the knot can diffuse a distance  $L \approx \sqrt{D_{knot} \tau}$ . We thus estimate a “processivity length” over which a tight knot diffuses, before opening up, by

$$L_p \propto a \exp(C \ell_B \lambda / a^2), \quad (7)$$

where  $C$  is a constant of order unity. The processivity length increases strongly with the screening length  $\lambda$  and quickly reaches a macroscopic length, indicating that the relaxation of a tight knot will be by diffusion along the chain, even for very long chains. Also note that  $L_p$  is in general much larger than the electrostatic persistence length which only grows quadratically with the screening length ( $\ell_c \approx \ell_B \lambda / a^2$ ).

## V. DISCUSSION

We have shown that long-ranged Coulomb forces generate a tension that tightens topological constraints into dense localized regions, leaving the rest of the polymer unentangled. For knots on ring polymers, we confirm the “factorization” of composite knots into their prime components. Tight knots remain, even when the Coulomb in-



teraction is screened, as long as the electrostatic contributions dominate the rigidity of the polymer. Once formed, tight knots drastically slow down the equilibration of the polymer (or polymer solution), as they typically relax by diffusion along the backbone. If the Coulomb interactions are strong enough, the knot is pulled so tight that it is unable to diffuse, and its position appears frozen. This is different from uncharged polymers where molecular dynamics simulations in ref. [37] find that tight knots in short uncharged polymers open up rapidly. Our results predict that tight knots in polyelectrolytes can be very stable and cause long relaxation times. While we have focused on single polymers, it is natural to speculate about similar behavior in solutions of many chains. It is indeed quite likely that *inter-chain* entanglements are also tightened in polyelectrolyte solutions and gels.

Additional consequences of tight knots are in their influence on mobility (electrophoresis), and on the mechanical strength of polymers. It has been shown recently by direct measurement on DNA and actin fil-

aments that knots significantly weaken the strand [6]. Similarly, molecular dynamics simulations of knotted polyethylene chains also find that the strands becomes weaker, and typically break at the entrance point where the straight segment ends and the tight knot begins [38]. Single stranded DNA is relatively fragile and sometimes breaks during electrophoresis or when subject to flow; tight knots may well be responsible for this phenomenon.

## VI. ACKNOWLEDGEMENTS

We thank Ralf Metzler and Andreas Hanke for helpful discussions. This work was supported by the National Science Foundation grants DMR-01-18213 and PHY99-07949, and by US-Israel Binational Science Foundation grant 1999-007. P.G.D. acknowledges support from the Research Council of Norway.

- 
- [1] P. G. de Gennes, *Scaling Concepts in Polymers Physics* (Cornell University Press, Ithaca, New York, 1979).
- [2] M. Doi and S. F. Edwards, *The Theory of Polymer Dynamics* (Clarendon Press, Oxford, 1986).
- [3] S. A. Wasserman and N. R. Cozzarelli, *Science* **232**, 951 (1986).
- [4] H. Wang, R. J. Di Gate, and N. C. Seeman, *Proc. Nat. Acad. Sci. (USA)* **93**, 9477 (1996).
- [5] N. C. Seeman *et al.*, *Nanotechnology* **9**, 257 (1998).
- [6] T. Arai, R. Yasuda, K.-I. Akashi, Y. Harada, H. Miyata, K. Kinoshita Jr., and H. Itoh, *Nature* **399**, 446 (1999).
- [7] K. Iwata and S. F. Edwards, *Macromolecules* **21**, 2901 (1988); K. Iwata and M. Tanaka, *J. Phys. Chem.* **96**, 4100 (1992).
- [8] S. R. Quake, *Phys. Rev. Lett.* **73**, 3317 (1994).
- [9] A. Y. Grosberg, A. Feigel, and Y. Rabin, *Phys. Rev. E* **54**, 6618 (1996).
- [10] Y. Rabin, A. Y. Grosberg, and T. Tanaka, *Europhys. Lett.* **32**, 505 (1995).
- [11] E. Guiter and E. Orlandini, *J. Phys. A* **32**, 1359 (1999).
- [12] V. Katritch, W. K. Olson, A. Vologodskii, J. Dubochet, and A. Stasiak, *Phys. Rev. E* **61**, 5545 (2000).
- [13] E. Orlandini, M. C. Tesi, E. J. Janse van Rensburg, and S. G. Whittington, *J. Phys. A* **31**, 5953 (1998).
- [14] O. Farago, Y. Kantor, and M. Kardar, *cond-mat/0205111*.
- [15] R. Metzler, A. Hanke, P. G. Dommersnes, Y. Kantor, and M. Kardar, *Phys. Rev. Lett.* **88**, 188101 (2002)[*cond-mat/0110266*]; and *Phys. Rev. E* **65**, 61103 (2002)[*cond-mat/0202075*].
- [16] E. Ben-Naim, Z. A. Daya, P. Vorobieff, and R. E. Ecke, *Phys. Rev. Lett.* **86**, 1414 (2001); M. B. Hastings, Z. A. Daya, E. Ben-Naim, and R. E. Ecke, *cond-mat/0110612*.
- [17] V. V. Rybenkov, N. R. Cozzarelli, and A. V. Vologodskii, *Proc. Natl. Acad. Sci. U. S. A.* **90**, 5307 (1993); S. Y. Shaw and J. C. Wang, *Science* **260**, 533 (1993).
- [18] M. C. Tesi, E. J. Janse van Rensburg, E. Orlandini, D. W. Summers, and S. G. Whittington, *Phys. Rev. E* **49**, 868 (1994).
- [19] B. Tinland, A. Pluen, J. Sturm and G. Weill, *Macromolecules* **30**, 5763 (1997).
- [20] Y. Kantor, M. Kardar, and D. R. Nelson, *Phys. Rev. Lett.* **57**, 791 (1986); and *Phys. Rev. A* **35**, 3056 (1987).
- [21] A. K. Trautwein, p. 353 in Ref. [23].
- [22] C. C. Adams, *The Knot Book: An Elementary to the Mathematical Theory of Knots* (W. H. Freeman and Co., New York, 1994).
- [23] *Ideal Knots*, K & E Series on Knots and Everything, vol. 19, ed. by A. Stasiak, V. Katrich and L. H. Kauffman (World Scientific, Singapore, 1998).
- [24] P. Hoidn, R. B. Kusner, and A. Stasiak, *New J. Phys.* **4**, 20.1 (2002).
- [25] J. Simon, p. 151 in Ref. [23].
- [26] R. B. Kusner and J. M. Sullivan, p. 315 in Ref. [23].
- [27] R. P. Grzeszczuk, M. Huang, and L. H. Kauffman, p. 183 in Ref. [23].
- [28] J. O'Hara, *Topology* **30**, 241 (1991).
- [29] P.-G. de Gennes, P. Pincus, R. M. Velasco, F. Brochard, *J. Phys. (Paris)*, **37** 1461 (1976).
- [30] P. Pfeuty, *J. Phys. (Paris)*, **39** C2-149 (1978).
- [31] G. Ariel and D. Andelman, *cond-mat/0112337*; and references therein.
- [32] L. D. Landau, E. M. Lifshitz, and L. P. Pitaevskii *Electrodynamics of Continuous Media* (Butterworth-Heinemann, Oxford, 1995).
- [33] T. Odijk, *J. Polym. Sci.* **15**, 477 (1977); J. Skolnick and M. Fixman, *Macromolecules* **10**, 944 (1977).
- [34] P.-G. de Gennes, *Macromolecules* **17**, 703, (1984).
- [35] P.-G. de Gennes, *Simple Views on Condensed Matter* (World Scientific, Singapore, 1998).
- [36] P.-G. de Gennes, *J. Chem. Phys.* **60**, 5030 (1974).
- [37] M. L. Mansfield, *Macromolecules* **31**, 4030 (1997).
- [38] A. M. Saitta, P. D. Soper, E. Wasserman, and M. L. Klein, *Nature* **399**, 46 (1999).